

**N93-19392**

**1992 NASA/ASEE SUMMER FACULTY FELLOWSHIP PROGRAM**

**JOHN F. KENNEDY SPACE CENTER  
UNIVERSITY OF CENTRAL FLORIDA**

**HYDROGEN LEAK DETECTION IN THE SPACE SHUTTLE**

<b>PREPARED BY:</b>	<b>Dr. Ronald G. Barile</b>
<b>ACADEMIC RANK:</b>	<b>Professor</b>
<b>UNIVERSITY AND DEPARTMENT:</b>	<b>Florida Institute of Technology Chemical Engineering Department</b>
<b>NASA/KSC</b>	
<b>DIVISION:</b>	<b>Engineering Design Lab</b>
<b>BRANCH:</b>	<b>Instrumentation &amp; Hazardous Gas</b>
<b>NASA COLLEAGUE:</b>	<b>Ric Adams</b>
<b>DATE:</b>	<b>August 31, 1992</b>
<b>CONTRACT NUMBER:</b>	<b>University of Central Florida NASA-NGT-60002 Supplement: 8</b>

## ACKNOWLEDGEMENTS

Every person below was a terrific help to me. This summer was a wonderful experience because of them.

The NASA persons who conceived and directed the project:

Ric Adams, who guided me with skill and patience, and his managers, Bill Helms and Dave Collins.

Other NASA persons who kindly gave of their time on a daily basis to help me along:

Bill Larson, Greg Hall, and Curtiss Ihlefeld.

The Boeing Haz Gas Lab personnel who put in a major amount of time and made all my computer and experimental work possible:

Larry Lingvay, Guy Naylor, Rich Hritz, Curt Lampkin and Terry Hammond.

Florida Tech Chemical Engineering student who did the last month's experiments and data reduction:

Dan Diolosa.

The Transducer Lab, Optics Lab and other Boeing personnel who helped substantially and loaned important equipment:

Drew Schmidt, Dick Deyoe, Jerry Mason, and Dr. Bob Youngquist.

Engineering Development and Test:

Stu Gleman, who is always happy to help by inventing a circuit or a gadget.

The KSC library staff gave efficient and kindly support.

The UCF administrators:

Dr. Loren Anderson and Carrie Stiles, courteous and capable.

THANKS!

## ABSTRACT

This study focuses on a helium gas jet flowing into room air. Measurements of helium concentration and velocity in the jet-air mixture are reported. The objective is to learn about jet characteristics so that dynamically similar hydrogen leaks may be located in the space shuttle. The hazardous gas detection system (HGDS) in the mobile launch pad uses mass spectrometers to monitor the shuttle environment for leaks. The mass spectrometers are fed by long sample tubes which draw gas from the payload bay, mid body, aft engine compartment and external tank. The overall purpose of this study is to improve the HGDS, especially in its potential for locating hydrogen leaks.

A rapid-response leak detection experiment was designed, built, and tested, following on the work done in this program last summer. The apparatus included a Perkin Elmer MGA-1200 mass spectrometer and air velocity transducer, both monitored by a Macintosh IIFX computer using LabVIEW software. A jet of helium flowing into the lab air simulated a gas leak. Steady helium or hydrogen-nitrogen jets were logged for concentration and velocity, and the power spectral density of each was computed.

Last year, large eddies and vortices were visually seen with Schlieren imaging, and they were detected in the time plots of the various instruments. The response time of the MGA-1200 was found in the range of 0.05 to 0.1 sec. Pulsed concentration waves were clearly detected at 25 cycles per sec. by spectral analysis of MGA data. No peaks were detected in the power spectrum, so in the present study, 10 Hz bandwidth-averaged power levels were examined at regular frequency intervals. The practical consequences of last year's study: sampling frequency should be increased above the present rate of 1 sample per second so that transients could be observed and analyzed with frequency response methods.

Many more experiments and conditions were observed in this second summer, including the effects of orifice diameter, jet velocity, sample tube design, radial effects, vertical flow, and low hydrogen concentration (1%). A frequent observation was

that the power spectrum, calculated from the Fourier transform of concentration fluctuations, gives a separate piece of information from concentration. Many of the tests suggest that power is high where mixing occurs at the helium-air interface. This fact is apparently independent of the concentration level, which could be high or low, but depends on the sample location relative to the jet (leak) origin. Whereas, high concentration may be due to a strong leak far away or a small leak close to the sample tube. If the power is low for any concentration level, this would signify helium is arriving at the sample tube by diffusion, not chaotic mixing caused by the jet interaction with air. The practical result is to propose a modification of the HGDL mass spectrometer data sampling and software so that sampling rates could be capable of observing at least 25 Hz fluctuations.

## SUMMARY

This study focuses on helium and hydrogen-nitrogen jets flowing into lab air. The technical goal is to learn about how leak jets break up and mix with air. Such information may be applied to analysis of helium signature tests or hydrogen leaks from the main propulsion system in the space shuttle. The hazardous gas detection system (HGDS) in the mobile launch pad uses mass spectrometers fed by long gas sampling tubes to monitor the payload bay, mid body, aft engine compartment and external tank. The mass spectrometers continuously assay the shuttle environment for hydrogen, helium, oxygen and argon. The overall purpose of this study is to improve the HGDS, especially in its potential for precisely locating gas leaks.

The motivation for this work is the difficulty experienced in the past when hydrogen leaks were discovered using the HGDS. The number of sample tubes is too small, i.e., five total, to give a detailed prediction of leak source and specific location. As it exists presently, the system can distinguish only broad areas such as payload bay, midbody, aft compartment, etc.

Last year the HGDS was reviewed and pre-existing leak data was analyzed for transients to determine if the concentration-time data had any . Spectral analysis was performed on earlier data measured at the OPF and in the Hazardous Gas Detection Lab. Then, a rapid-response leak detection experiment was designed, built, and tested. The apparatus included a Perkin Elmer MGA-1200 mass spectrometer, an air velocity transducer, and a pressure transducer, all monitored by a Macintosh IIFX computer using LabVIEW software. A jet of helium flowing into the lab air simulated a gas leak. Schlieren imaging and video recordings were also employed to study the flow phenomena. Experiments on leak jet character-ization included velocity, pressure and concentration profiles and in particular on spectral analysis of these signals. Steady and pulsed jets were logged for concentration, velocity, and pressure, and the power spectral density was computed for each observation.

The LabVIEW software performed well in both analysis of earlier data and in real-time data acquisition and reduction. The air velocity transducer (TSI) and the pressure transducer

(Rosemount) were capable of measuring rapid transients in helium jet phenomena, and they have the versatility and potential to be applied to leak detection and location. Particular emphasis was centered on large eddies and vortices in the jet-air mixing zone. Large eddies and vortices were visually seen with Schlieren imaging, and they were detected in the time plots of the various instruments. The response time (63.2%) of the MGA-1200 was found in the range of 0.05 to 0.1 sec. Pulsed concentration waves were clearly detected at 25 cycles per sec. by spectral analysis of MGA data. For certain, the MGA was fast enough to detect transients such as hydrogen or helium eddies in the time trace data, if sampled at 50 Hz. Spectral analysis showed some evidence of correlated power in the 0.1 to 20 Hz. region, but visual and transient concentration observations indicated that eddy shedding from the leak jet was somewhat irregular in time. Thus, such events did not correlate well as definite peaks in power spectral density plots. One practical consequence of that study was to suggest that the backup HGDS sampling frequency should be increased above the existing rate of 1 sample per second.

The second year study focused on a refined spectral analysis of concentration and velocity data. The basic apparatus was reassembled in the configuration described above. LabVIEW software was extended to include band width averaging at selected central frequencies, e.g., 10 Hz bandwidths at center frequencies of 5, 10, 15 Hz, etc. Three sample tube designs were studied, two orifice types, gas flows of 3.64 to 14.56 SLM using 99.999% helium or 1% hydrogen in nitrogen. Concentration and spectral density were obtained at various axial lengths downstream from horizontal jets, including the centerline and various radial positions to the side and above the jet axis. Flow obstructions were also placed into the jet axis downstream from the origin. The general result is that concentration and power calculated from concentration fluctuations give distinct information about where the sample tube is relative to the leak jet origin. In the vicinity of the leak origin, one finds high or low concentration depending on the leak strength and the purge gas rate. But, in this region there is likely to be peaks in power independent of the concentration. Thus, mass

spectrometers should be operated at a high sampling rate, e.g., 25 Hz, so that power may be determined. This would result in greater capability to detect gas leaks and infer the leak location.

## TABLE OF CONTENTS

- I INTRODUCTION
  
- II BACKGROUND
  - 2.1 Present System Definition
  - 2.2 Earlier KSC Work Related to Hazardous Gas Detection
  - 2.3 Literature Survey of Jets
  
- III APPARATUS AND PROCEDURE
  - 3.1 LabVIEW Software
  - 3.2 Apparatus and Data Acquisition
  - 3.3 Procedure
  
- IV RESULTS AND DISCUSSION
  - 4.1 Simulated helium leaks
  
- V CONCLUSIONS AND RECOMMENDATIONS

REFERENCES

FIGURES

## LIST OF ILLUSTRATIONS

### Figure

1. Jet review.
2. Present apparatus showing sample tube 3 arrangement.
3. a) GHe concentration and power vs. x. Sonic orifice jet, 3.64 SLM, ST1; b) GHe concentration vs. time, sec., at 7 values of x, 0 to 24 in; c) GHe power vs. time, sec., at 7 values of x, as in Fig. 3b.
4. a) GHe concentration and power vs. x. Tygon tube jet, 3.64 SLM, ST1; b) GHe concentration and power vs x. 1/4 in. Tygon tube jet, 3.64 SLM, replicate.
5. Helium concentration vs. length, Tygon tube at 3 flows (ST1). 3.64, 7.28, 14.56 SLM GHe.
6. Helium concentration and power vs. x. Comparison of small (S.O.) and large (Tygon) orifice at 3.64 SLM.
7. Power vs. length and frequency. Power is 10 Hz bandwidth-averaged at center frequencies shown on top graph.
8. Mechanical chopper at 25 Hz placed in jet stream 3 in. from orifice.
9. Concentration and power at 5 Hz vs. distance. Comparison of GHe, O<sub>2</sub>, and N<sub>2</sub>. ST3, S.O., 3.64 SLM GHe.
10. Velocity and 5Hz-power vs. x. Comparison of GHe, O<sub>2</sub>, and AVT. ST3, sonic orifice, 3.64 SLM GHe.
11. Concentration and velocity vs. distance. Comparison of 3.64 and 7.28 SLM GHe. ST3, sonic orifice.
12. Power at 5 Hz. vs. length. Comparison of GHe and AVT data. ST3, sonic orifice, 7.28 SLM.
13. Helium concentration at three x values vs. radial coordinate, y.
14. Power at 5 Hz, three x values, vs. y.
15. Concentration and power at 5 Hz vs. length. ST3, sonic orifice, 3.64 SLM GHe.
16. Concentration and power vs. length. Horizontal cylinder obstruction at x=1 in. ST3, sonic orifice, 3.64 SLM GHe.
17. Concentration and power vs. length. Horizontal cylinder obstruction at x=1 in. ST3, sonic orifice, 7.28 SLM GHe.
18. Top: helium (ppm) signature test in shuttle MPS; middle: helium (%) stream direct to mass spectrometer vs. time, sec.; bottom: stagnant lab air (%) vs. time, sec.

## I INTRODUCTION

In the space shuttle, hydrogen and oxygen are the main engine propulsion gases, as well as the fuel-cell power system gases. Leaks of these gases may be found in the aft fuselage, the mid body, and other areas. Various forms of leak detection equipment are employed in and around the shuttle wherever hazardous materials are present. The hazardous gas detection system (HGDS) uses mass spectrometers fed by long gas sampling tubes to monitor the payload bay, mid body, aft engine compartment, and external tank. The mass spectrometers in the HGDS monitor the environment for hydrogen, helium, oxygen, nitrogen and argon.

This study will focus on helium jets in the lab which are intended to represent a typical leak during tests of the main propulsion system (MPS). Helium signature tests are routinely performed to determine the shuttle's MPS integrity. These tests, involving pressurization of the MPS with GHe and monitoring for helium leaks with the HGDS, are scheduled at the launch pad previous to the start of countdown. Hydrogen or oxygen leaks may still occur during tanking operations after the helium signature test is acceptable. These would be detected by either catalytic hydrogen detectors situated outside in the tank-piping system, or by the prime, backup, or external tank (HUMS) mass spectrometers sampling around and in the shuttle. By studying jets with a mass spectrometer using frequency response techniques, new understanding gained will lead to better methods for detecting and locating leaks in the MPS.

### Main Goals of the Two-Summer Study:

1. Assess the present HGDS and analyze earlier leak data to determine if leak data has frequency information which can lead to pinpointing the leak location .
2. Design, build, and test a rapid-response leak detection experiment which focuses on leak characterization including velocity, pressure and concentration profiles and in particular on rapid fluctuations and spectral analysis of these variables.
3. For a longer-term objective: Predict an improved placement of sample tubes and improved data analysis for special tests so that leak locations can be pinpointed.

## II BACKGROUND

### 2.1 PRESENT SYSTEM DEFINITION

The hazardous gas detection system at KSC is a mix of UTI (quadrupole) and Perkin Elmer (fixed sector) mass spectrometers. They monitor the shuttle and tail service mast (both prime and backup HGDS), and the external tank (HUMS). Gas samples are drawn through 0.18-in. ID tubes to mass spectrometers situated 100 to 200 ft. away inside the mobile launch platform. Five gas samples are sequentially assayed for hydrogen, helium, oxygen, nitrogen and argon. The five samples arrive in separate tubes: three from the shuttle, one from the tail service mast, and one from the external tank.

Sample gases are drawn from the shuttle interior into 0.23-in. ID SS tubes distributed in the aft area. The payload bay and mid body tubes are located just aft of the 1307 bulkhead. Four tubes which sample the payload bay purge are connected through tees into one tube which is routed through the umbilical disconnect panel (UDP, line 2). Two SS tubes which sample the mid body purge are connected into one tube leading to the UDP (line 4). The pair of aft sample tubes are mixed together and routed to the UDP. The aft sample tubes are located several feet aft of the 1307 BH at the #9 vent doors, thus the aft sample could reflect upstream leaks from the MB and PLB.

A 180-lb/min. nitrogen purge is flowing at the pad when the cryogenic propellants are loaded into the vehicle. Both hydrogen and oxygen flow inside separate piping systems from the tail service mast to the shuttle aft compartment to the external tank. Before loading cryogenics, a test is done by injecting helium in this piping system, the main propulsion system (MPS), with air purge on the outside (1). Hence, leaks in the cryogenic piping can be detected via helium tests before loading cryogenics, and by hydrogen and oxygen detection during and after these are loaded on board. Due to safety considerations, the present study was done primarily with helium, although hydrogen can be easily implemented in future work.

### 2.2 EARLIER KSC WORK RELATED TO HAZARDOUS GAS DETECTION

In 1990, Schleier studied gas leaks of helium, nitrogen, and

argon by flowing the gases through a slightly cracked gate valve (2). Using helium at 68 psig and 105 sccm as the reference condition, flows of helium, nitrogen, and argon correlated well as predicted vs. observed flows. Mehta characterized a turbomolecular-pumped magnetic sector mass spectrometer in 1988 working with the HGDL (3). The model was Perkin Elmer MGA-1200, the same type which is employed in the present study (H2S2). Linearity, precision, drift, detection limits and accuracy were found to be acceptable for quantitative analytical determination of hydrogen, helium, oxygen and argon in nitrogen or helium background gases. The 90% rise times for pulse inputs were on the order of one-half second.

One-second pulse of nitrogen into helium put into the Perkin Elmer 17" disconnect mass spectrometer resulted in an 84% peak on nitrogen and a total dead and lag time of less than 0.1 sec on the upswing (4). The downswing started about 0.2 sec late, and took another 0.8 sec. to drop to zero. A one-second pulse of helium into nitrogen rose quickly to 98% in less than 0.1 sec., but it did not fall off from 98% until 3 sec. and it zeroed after another second (4 sec. total). A recent internal HGDL study (5) on noise in MGA-1200 reported that the unfiltered 60-cycle and related harmonic rms noise level was on the order of 100 mV. Part One of the present study, completed in summer 1991 (6), is reviewed in the present document.

### 2.3 LITERATURE SURVEY OF JETS

Last summer, a wide-ranging review of jets, mass spectrometers, gas leaks, etc., was presented (6). The survey below focuses on earlier and new references which pertain to frequency and mixing phenomena.

A survey of jet literature was performed because a gas leak behaves similarly to a jet with regard to velocity decay, pressure profile, concentration decay, sonic waves, etc. The fluctuations seen in mass spectrometer test data are reminiscent of vortices or large scale eddies which form at the edge of the jet-air mixing zone (7-12). These swirling structures, which travel with the jet at roughly the local centerline velocity, could give rise to the type of concentration fluctuations which are observed in MS tests of concern here.

A small laminar or turbulent fluid stream issuing into a large region containing the same or similar fluid at rest is termed a free (submerged) jet, Fig.1 (top) (13). For a laminar free jet, there is an orderly pumping action by the jet, resulting in both lateral and axial motion in the surrounding fluid. The difference in velocity between a free jet and its surroundings generates a diffusion (mixing) region characterized by large scale eddies. Vortices occur in the interface region between the central jet core and the surrounding fluid. Vorticity (need Defn) tends to agglomerate, forming large-scale eddies, which grow by entraining fluid from the surroundings and by pairing-- the basic mechanism or the growth of the shear mixing layer. While eddy motion is similar to molecular motion, there are important differences. Turbulent movement depends on the general (directed) motion and requires a continuous supply of energy to maintain it, while molecular motion does not. The source of energy which supports the eddies is the directed kinetic energy of the jet which eventually is transformed to kinetic energy of turbulence. The turbulence, in turn, decays irreversibly through viscous shear.

The free jet spreads because of shear at its boundaries, and the total flow crossing successive normal planes increases because of entrainment of the surrounding fluid, Fig. 1 (middle) (14). Of course, continuity must be satisfied, thus the increasing flow area requires a decreasing jet velocity. The mixing region, emanating from the solid boundary of the jet, progresses both inward and outward with respect to the jet axis as a function of axial distance. However, close to the exit plane of the jet there exists a region called the potential cone or core which is not disturbed by the large eddies. Downstream from the potential cone, the entire central portion of the jet is filled with large-scale eddies (once the diffusion has reached the axis) and the flow is fully established.

The momentum of a jet issuing from a circular orifice is:

$$M_o = (\rho \cdot A_o \cdot V_o) \cdot V_o.$$

where

$\rho$  = density

$A_o$  = orifice area

$V_o$  = velocity at orifice.

To a good approximation, momentum is conserved, thus, the

product ( $\rho \times V_0$ ) must remain constant by the jet area expanding and the velocity slowing down as it flows downstream. Dynamic similarity or similarity solutions generally apply to the free jet. This predicts the result that dimensionless profiles of mean velocity in the diffusion (mixing) region must be defined by the same functional form at all sections normal to the flow (Fig. 1, bottom) (14):

$$V_x/V_{max} = f(N)$$

where

$$N = l^*/g(x)$$

$l^*$  = radial coordinate measured out from the edge of the mixing region

$g(x)$  = arbitrary measure of radial extent of diffusion region (similarity).

Practically, similarity means that all velocity profiles of a given flow field will fall on one single curve. Three simple results of various studies are:

1.  $g(x) = C * x$ .
2.  $V_{max}(\text{centerline})/V_0 = x_c/x$ , where  $x_c$  is the length of the central core.
3. The data for  $f(N)$  is reasonably fit by the error function.

Measurements of the mixing of two coaxial hydrogen-air jets are reported by Chriss (15), including centerline decay and radial profile shapes of composition, velocity, and total enthalpy. The striking result is that velocity and composition decay almost identically on dimensionless plots. These plots verify that velocity profiles fit the similarity condition, but in addition the concentration profiles also have this property. Becker et al. (7) worked with an air-air jet marked with oil smoke. Turbulent concentration fluctuations of the nozzle gas diffusing into the stagnant gas were on the order of 25% of the centerline value (lateral distance from centerline about 1/3 of jet radius). Heat transfer and flow measurements including frequency and intermittency data are given by Chua and Antonia (8). Turbulent fluctuations ranged from 10Hz for large peaks to 100 Hz for small variations.

Detailed analysis of shuttle hydrogen leaks are given by Seymour (16) on the STS-35 scrub-3 hydrogen leak analysis. The study featured a transient model of the aft compartment H<sub>2</sub> concentration. The basic time constant of the aft compartment purge flow is about 90 sec. Some of the major conclusions were: the leak did not exist at ambient temperature, the engine pre valve 2 was the most likely leak location, at least 80% of leakage came from the engine 2 pre valve, the scrub-2 leak area was twice that of scrub 3 and consistent with the known engine 3 pre valve detent cover seal leakage, and leak area changes cannot be inferred from concentration changes without employing an analysis similar to that used in the study, i.e., the compartment model. The above work may be more readily understood by referring to MPS diagrams for propellant flow, etc. (17,18).

### III APPARATUS AND PROCEDURE

#### 3.1 LabVIEW SOFTWARE

LabVIEW programs (VI's) written by Larry Lingvay (Boeing HGDL) were used to get and analyze helium leak data. The data were stored in files such as MacPaint and as tab-delimited text files. The latter could be read by other LabVIEW software such as *Band Width Integrator* and *Data Display VI*. The software used in this project along with their functions are:

1. Super Spectrum Analyzer (SSA)--Collect helium concentration data, calculate the average over one or more seconds, take power spectrum of concentration data, display plots of concentration and power. Similarly, other gases could be measured by switching VI controls. The air velocity transducer (AVT) was also connected to SSA, on channel 5. A data file is generated which is read into Multifile Integrator (below).

2. Analog Mass Spec--Collect hydrogen, helium, nitrogen, oxygen and argon data at 1 sec. intervals as in IHUMS system.

3. Multifile Integrator--Take power spectrum vs. frequency data from SSA-generated files and integrate at several center frequencies, e.g., 5, 10, 20, 40, etc., for 10 Hz band widths. Each file is measured at a different length or position in the jet.

4. Data Multiplot Display--Plot integrated power data vs. length for various center frequencies.

#### 3.2 APPARATUS AND DATA ACQUISITION

The apparatus and data system were similar to last year. Changes included new sample tube designs and new experimental configurations. A helium leak was simulated in the HGD Lab by a pure helium stream (KSC grade) flowing from the lab-service panel through 1/32-in. ID stainless steel tubing, and exiting through a small nozzle or a 1/4-in. ID Tygon tube. The gas exited the nozzle from a circular orifice, 0.05 cm. diameter, recessed in a short tube, 0.5 cm long and 0.4 cm. diameter (sonic orifice). In effect, the jet was actually emerging from the 0.05-cm. tube at or below local sonic velocities, depending

on the upstream pressure.

A schematic drawing of the equipment used in the HGDL is shown in Fig. 2. A Rosemount pressure transducer was used to measure pressure fluctuations in the jet field (Minneapolis, MN). This device is capable of measuring pressure from 22 to 32 inches of mercury absolute. Velocity and its fluctuations were detected by a TSI Inc. air velocity transducer (AVT) with a range of 0 to 10,000 fpm (St. Paul, MN). These probes were mounted on a small vise which was placed at various measured locations in relation to the jet origin.

The jet stream representing the leak was measured and controlled by a Sierra Instruments 840 SideTrak mass flow meter/controller. The instrument was calibrated for nitrogen gas flow, but was correctable to helium gas by multiplying the reading by 1.453 (for units of standard liters per minute, SLM). An independent check on the frequency response of velocity and concentration measurements was provided by installing in the leak jet a mechanical chopper used in optical experiments.

A Perkin Elmer MGA-1200 (H<sub>2</sub>S<sub>2</sub>) mass spectrometer was employed as the gas analyzer. The helium jet was sampled with a 15-ft length of 1/32-in ID stainless steel tubing with a crimp at about 3 inches downstream from the sample orifice. This tube, *ST1*, was connected directly to the porous plug at 200 Torr in the MS evacuated area, and as such it was pumped directly with the MGA roughing pump. Samples were taken at various locations downstream from the jet origin normally in the horizontal direction, *x* (*x*=axial, *y*=lateral-horizontal, *z*=vertical). Data were taken with this tube between 7-13-92 and 7-24-92. Later, the same tube minus the crimped region, became a 14.5-ft. length of 1/32-in. ID SS capillary tubing, which was fitted to the MGA inlet valve #3. This tube, *ST2*, was also pumped by roughing pump as with *ST1*. The crimp was cut off due to plugging, as manifested by slow sample tube response and recovery. Flow resistance in valve #3 was sufficient to provide enough pressure drop so that the vacuum system was not overloaded. The measured time constant of this second tube was about 0.08 sec.

After a few trial runs, *ST2* was found to be inappropriate for lab air measurements. A third change (*ST3*, on 8-7-92) employed the 14.5-ft 1/32-in ID tube connected directly into the heated

MGA valve #1, with a vacuum pump at the valve outlet. In this way, flow in the sample tube remained high, with a small leak sample drawn off a tee to the mass spec. This insured that the transit time through the sample tube was high, but the pressure to the mass spec remained low. (The big pressure drop in the sample line occurred in capillary tube downstream from the valve.) The sampling dead time was a few seconds.

All sensors were fed into a National Instruments data acquisition board (NB-MIO-16XL-42) plugged into a MacIntosh IIFX computer. A VI called *Super Spectrum Analyzer* sampled, plotted and analyzed the data from each sensor. The analysis routine was to sample during a given time window with a specified period of samples, e.g., 1 or 2 sec., for a specified band width of typically 100 Hz. The mean concentration was computed, and the time traces of concentration and power spectrum were plotted, all in the LabVIEW panel. Then, the frequency data were integrated (offline) about selected center frequencies for 10 Hz band widths by a VI called *Multifile Integrator*. Data generated in *Multifile Integrator* were then displayed by *Data Multiplot Display* as average power vs. jet axial length,  $x$ , as a function of several center band frequencies.

### 3.3 PROCEDURE

Set gas flow, put sample tube and/or AVT in vise at specified location. Calibrate mass spec zero and span gas, run LabVIEW, store data in file, save paint file of LabVIEW screen. Run data analysis VIs, create plots of concentration and power spectra.

## IV RESULTS AND DISCUSSION

### 4.1 SIMULATED HELIUM LEAKS

The experimental variables were helium jet flow rate, 3.64, 7.28, and 14.56 SLM; jet orifice either sonic orifice or 1/4 in.-ID Tygon tube; sample tubes ST1, ST2, and ST3; various axial positions from 1/16 to 36 in.; and, radial positions at fixed x; horizontal, cylindrical bar obstruction, 3/4-in. diameter, 3/4" downstream from jet; jet orientation to gravity was usually horizontal, but vertical up flow was also observed with/without fan-driven crossflow.

4.1.1 SAMPLE TUBE 1. Experiments using sample tube 1 (ST1) were run between 7-13-92 and 7-24-92. Individual experiments are discussed below in order of the run date.

7-13-92 Fig. 3a shows the percent helium and the hand-averaged power due to concentration fluctuations at several frequencies versus axial length downstream. For this slow flow, 3.64 SLM (3,640 SCCM) helium, the concentration of helium falls very quickly from 100% at the jet origin to 2.5% at  $x = 6$ ". (At this rate, the helium exits the 0.4 cm diameter orifice into air at 1035 FPM.) In contrast, the power at 5 Hz rises up from -31 near the jet to -4 at  $x = 3$  and 6 in. downstream (relative log scale units, analogous to dB if the concentration were in volts). Higher frequencies, also shown on Fig. 3a, follow the same trend with a power peak in the 3 to 6 in. range. There is also evident a progressive downward trend of power as frequency increases in steps to 100 Hz. The background air in the lab has a flat power spectrum of -60 to -80 for all frequencies between 5 and 100 Hz. Figs. 3b and 3c show the concentration record and power vs. frequency during the above runs which were 1 second in duration. Average helium concentration during this period is noted on the individual traces at various  $x$  values.

7-16-92 to 7-24-92 A series of runs was observed with 1/4-in. ID Tygon tubing as the jet orifice. The helium flow was 3.64 SLM or 412 FPM issuing from the tube. A plot of percent helium and power versus length for Tygon is remarkably similar to the sonic orifice plot, Figs. 4 and 3a, respectively. A replicate run is shown in Fig. 4b. The key differences between the sonic orifice and the Tygon are 1) the Tygon orifice produces a slower

jet which decays in concentration faster, i.e., within 3 inches, and 2) the power peak for Tygon occurs closer to the origin, 1 in. instead of 3 to 6 in. as with the sonic orifice. The helium flow was subsequently doubled to 7.28 SLM (824 FPM) and doubled again to 14.56 SLM (1650 FPM) in order to show the effect of flow rate on these phenomena. A combined plot is shown in Fig. 5. As expected, higher flow stretches out the concentration profile to higher values downstream. The power peaks move downstream and are flattened as flow rate is increased. Fig. 6 shows the effect of two different orifice types at the same flow rate. The sonic orifice has an area of 0.00196 sq. cm. at the smallest point compared to the tygon tube which is 0.317 sq. cm. in cross section. Thus, there is an initial velocity ratio of 162 for the sonic orifice vs. the Tygon tube. This physical difference gives rise to similar sharp concentration drops within 6 in. downstream, but the power signatures are much different.

4.1.2 SAMPLE TUBE 2. With the crimp removed, this sample tube seemed more responsive. However, it was used only two days because its connecting valve arrangement was not providing enough pressure drop prevent saturation of the turbomolecular vacuum pump.

8-4-92 Again at 3.64 SLM helium flow with the sonic orifice, there was a pronounced power peak in the vicinity of 6 inches downstream, Fig. 7. The concentration profile was stretched out downstream to give higher concentration of helium, possibly due to the new sample tube arrangement. For example, the jet was 4.4% helium at 12 in. downstream, as opposed to 0.84% at the same location using ST1.

A mechanical-optical chopper was inserted into the jet at  $x=1$  in. in order to introduce a known frequency of concentration variation. The jet was sampled at about  $x=3$  in. The chopper was set at 25 and 15 Hz. Both settings gave pronounced power peaks at the respective frequencies. The former concentration and power curves are shown in Fig. 8.

4.1.3 SAMPLE TUBE 3. This change slowed the apparent response by a small amount. The response time was checked using a paper card to block the sample tube and then quickly remove it. A time trace of concentration showed that the response time

constant (63.2% of total rise) was about 0.16 sec, still a fast response.

8-7-92 A series of experiments was designed to show concentrations and power of oxygen and nitrogen from the surrounding air along with the usual helium record. Concentrations of these gases are shown in Fig. 9, top. Note this figure has only three x locations, but it shows that the data are basically consistent, i.e., helium drops off to zero percent at 24 in., oxygen rises to 21%, and nitrogen rises similarly. However, nitrogen is 5 to 10% low due to a mass spectrometer calibration anomaly. Fig. 9 also shows the power level for these gases versus x. The nitrogen power is about ten relative units above helium, and the helium power is about 5 units above oxygen. Although helium concentration is low at 12 in., the power level persists at a high value, showing decoupling of concentration and power.

8-11-92 This experiment extended the previous run of 8-7-92, with the inclusion of the air velocity transducer (AVT) to measure an approximate local velocity. Helium and oxygen concentrations, and stream velocity are plotted in Fig. 10. The velocities at small distances downstream are low by 10 percent or less due to the error introduced by measuring a helium-air stream with an air-calibrated AVT. This error becomes negligible past x=10 in. where helium falls to a few percent. The AVT power at 5 Hz does not have a peak downstream like concentration. This was not due to limitations in frequency response of the AVT, however. This instrument was observed by the author to have very fast response, at least capable of seeing 20 Hz waves, last year (6). The AVT, oxygen and helium power traces in Fig. 10 clearly indicate although helium is rapidly diluting and oxygen is climbing, the power levels are similar and actually are reversed for these gases (helium is higher).

8-12-92 All conditions were repeated from 8-11-92 except the helium flow was doubled to 7.24 SLM. Fig. 11 shows the effect of flow on concentration and velocity. Higher velocity stretches the jet out downstream so that concentration is elevated by a few percent at 10 in. The velocity effect is more pronounced. Fig. 12 shows the difference between helium power and AVT power at 7.28 SLM. The effect of flow on power at 5 Hz

may be ascertained by comparing Figs. 10 and 12. Helium power is similar close to the origin, but it remains elevated at 24 in. and beyond when the velocity is higher.

8-13-92 This run repeated the experiment of 8-11-92 at 3.64 SLM with the additional feature of including radial measurements for three  $x$  locations. Data were observed on the horizontal plane to the right ( $+y$ , looking downstream) of the jet plane. Concentration profiles in Fig. 13 clearly show how the jet spreads out by the increase in helium concentration laterally as the jet moves downstream. The power levels present a similar picture where the high power levels downstream indicate intense concentration fluctuations for  $x=6$  in. at  $y=0.125$  to 1 in., and for  $x=12$  in. at  $y=0.125$  to 3 in. Again, power and concentration have different trends with  $x$ , e.g., at  $x=6$  in.

8-14-92 Similar to 8-13-92, this series was designed to show the effect of  $+z$  variations at 2, 4, and 6 in. above the jet. Fig. 15 shows that the jet is spread considerably in the vertical direction at  $x=12$  in., where a concentration peak occurs. The power peaks occur at different locations.

8-17-92 For 3.64 SLM helium flow, a run was made using a horizontal, 3/4-in. diameter aluminum cylinder to block the jet. The cylinder was placed with its center at  $x=1$  in. Concentration and power were observed at 6  $x$  locations for 4  $z$  values between 0.5 and 6 inches, Fig. 16. An interesting feature of these data is that power and concentration do not follow analogous curves. For example, at  $x=6$  in., the percent helium for  $z=0, 0.5$ , and 1 in. are all much reduced from their upstream values, but their power levels are similar. This means that power gives a separate piece of information from concentration. It suggests that power is high where mixing occurs at the helium-air interface, whereas high concentration may be due to a strong leak far away or a small leak close by but with the sample tube outside of the flow and mixing area. The latter case would signify helium is arriving at the sample tube by diffusion, not chaotic mixing caused by the jet interaction with air. Comparison with Fig. 3a (5 Hz, no obstruction) shows that near the obstruction, power levels are similar, but downstream the power is very low in the wake of the obstruction. Elevated concentration levels are seen above the jet in the wake of the

obstruction, but these are absent in Fig. 15 (no obstruction).

8-18-92 This run was like 8-17-92, but with a double helium flow of 7.28 SLM, Fig. 17. Doubling the flow reduces the near-field concentration by a factor of two (around  $x=6$  in.), but helium concentration is ten times higher than for the slower flow at  $x=12$  in. Also at  $x=12$  in., power remains high while concentration falls off rapidly.

8-25-92 to 8-27-92 These runs include a replicate of earlier helium experiments at 3.64 SLM GHe, sonic orifice, but with 1% hydrogen in nitrogen as the gas jet at 2.5 SLM, using ST3 (note that this needs to be rerun at 3.64 SLM); and, vertical upflow with and without crossflow provided by a small fan. At final writing, results were not available, but will be communicated privately to Ric Adams.

4.1.4 OTHER EXPERIMENTS. This study was prompted in part by strongly fluctuating data obtained in earlier experiments in the HGDL and in helium signature tests. For example, data from a shuttle MPS LO2 helium signature test are shown in Fig. 18. These data are sampled at about 1 sec. rate and show puzzling fluctuations. To shed some light on this problem, pure helium was flown directly to ST1 at atmospheric pressure, indicated as % helium. Fig. 18 shows these in the middle for comparison including both helium and nitrogen concentrations at 1-sec. intervals (nitrogen leaked in). The bottom of this figure shows stagnant lab air analysis, percent nitrogen and oxygen. All of these figures look similar, suggesting that the fluctuations may be inherent in the mass spectrometer. There is no other apparent reason for the concentrations to vary when the gas is directed at the sample tube without any flow or mixing phenomena present.

## V CONCLUSIONS AND RECOMMENDATIONS

### Conclusions

- \* The helium jet behaves as predicted from the literature in terms of rapid concentration and velocity decay, and the lateral spread of mass and momentum.
- \* The great majority of runs showed that local concentration and power levels were independent. Typically, power had peaks in regions where concentration was rapidly decaying.
- \* The effect of orifice size was to increase velocity at constant flow for a smaller orifice resulting in stretched-out concentration profiles and higher power traces.
- \* Sample tube design has a reasonably strong effect. All three tubes had time constants less than 0.2 sec., the last (ST3) having the largest of 0.13 to 0.16 sec. A small bore gives the advantage of a short transit time without damping frequency information.
- \* AVT power did not correlate well with concentration power despite the rapid response capability of the AVT.
- \* Radial measurements indicated a distinction between concentration and power also.

### Recommendations

- \* One practical consequence of this study is to suggest that the backup HGDS sampling frequency should be increased above the present rate of 1 sample per second.
- \* Also, it would be interesting to do tests like the above using two or more mass spectrometer sample tubes at different locations. These could be monitored sequentially by switching a solenoid valve between tubes. Then, spectral analysis of different tube locations would be analyzed for transient events pointing to the leak location. Such a system could be implemented with the present HGDS sample tubes in the shuttle.

## REFERENCES

1. Bilardo, V. J., Jr., and Izquierdo, F., "Development of the Helium Signature Test for Orbiter Main Propulsion System Revalidation Between Flights," AIAA 25th Aerospace Sciences Meeting, Jan., 1987.
2. Schleier, H., "Correlation of Leak Rates of Various Fluids with the Leak Rate of an Inert Gas in the Same Configuration," NASA/ASEE Summer Faculty Fellowship Program, 308-338, 1990.
3. Mehta, N. K., "Characterization of a Turbomolecular-Pumped Magnetic Sector Mass Spectrometer," NASA/ASEE Summer Faculty Fellowship Program, KSC/UCF, 1988.
4. Kachnic, J., and Raisin, P., "The 17" Disconnect Mass Spectrometer with Turbomolecular Turbo Pump," Internal Report from Boeing to Dave Collins, NASA-KSC, DL-ESS-24, 4-12-88.
5. Hazardous Gas Detection Lab, Internal Report, "Overview of MGA-1200 Electrometer Card Testing," 1990.
6. Barile, R. G., "Hazardous Gas Leak Analysis in the Space Shuttle," NASA/ASEE Summer Faculty Fellowship Program, KSC/UCF, 1991.
7. Becker, H. A., Hottel, H. C., and Williams, G. C., "The Nozzle Fluid Concentration Field of the Round Turbulent Free Jet," J. Fluid Mech., 30, 285-303 (1967).
8. Chua, L. P., and Antonia, R. A., "Flow Reversal and Intermittency of a Turbulent Jet," AIAA J., 27, (11), 1494-1499 (1989).
9. Ghoniem, A. F., Chen, D. Y., and Oppenheim, A. K., "Formation and Inflammation of a Turbulent Jet," AIAA J., 24, (2), 224-229 (1986).
10. Lam, K. M., and Ko, N. W. M., "Investigation of Flow Structures of a Basic Annular Jet," AIAA J., 24, (9), 1488-93 (1986).
11. Birch, A. D., Brown, D. R., Dodson, M. G., and Thomas, J. R., "The Turbulent Concentration Field of a Methane Jet," J. Fluid Mech., 88, (3), 431-449 (1978).
12. Yule, A. J., "Observations of Late Transitional and Turbulent Flow in Round Jets," in Turbulent Shear Flows, Durst (Editor), Univ. Park, PA, Apr. 18-20, 1977.
13. Schlichting, H., Boundary Layer Theory, McGraw-Hill, 1960.

14. Benedict, R. P., "The Flow Field of a Free Jet," in R. B. Dowdell, Ed., Flow-Its Measurement and Control in Science and Industry, Vol. 1, ISA, 1974.
15. Chriss, D. E., "Experimental Study of Turbulent Mixing of Subsonic Axisymmetric Gas Streams," Arnold Engineering Development Center, AEDC-TR-68-133, Aug. 1968.
16. Seymour, D., "STS-35 Scrub 3 Hydrogen Leak Analysis," NASA TM-103548, July, 1991.
17. "MPS-2102, Main Propulsion System Workbook," Advanced Training Series, JSC-ATS-MPS-2102, July, 1983.
18. "Integrated System Schematic, Main Propulsion System," Orbiter Vehicle, V572-941099, Rockwell International Corp., Space Div.

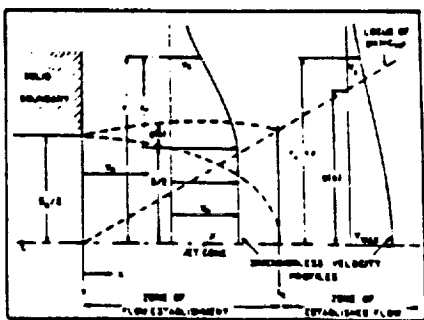
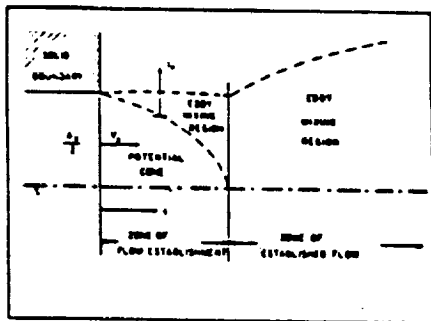
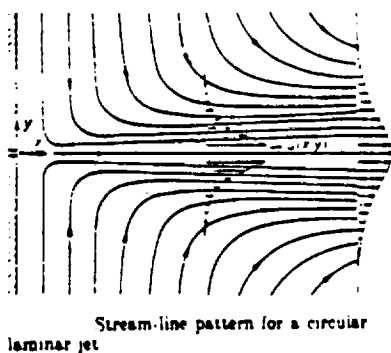


Figure 1. Jet review.

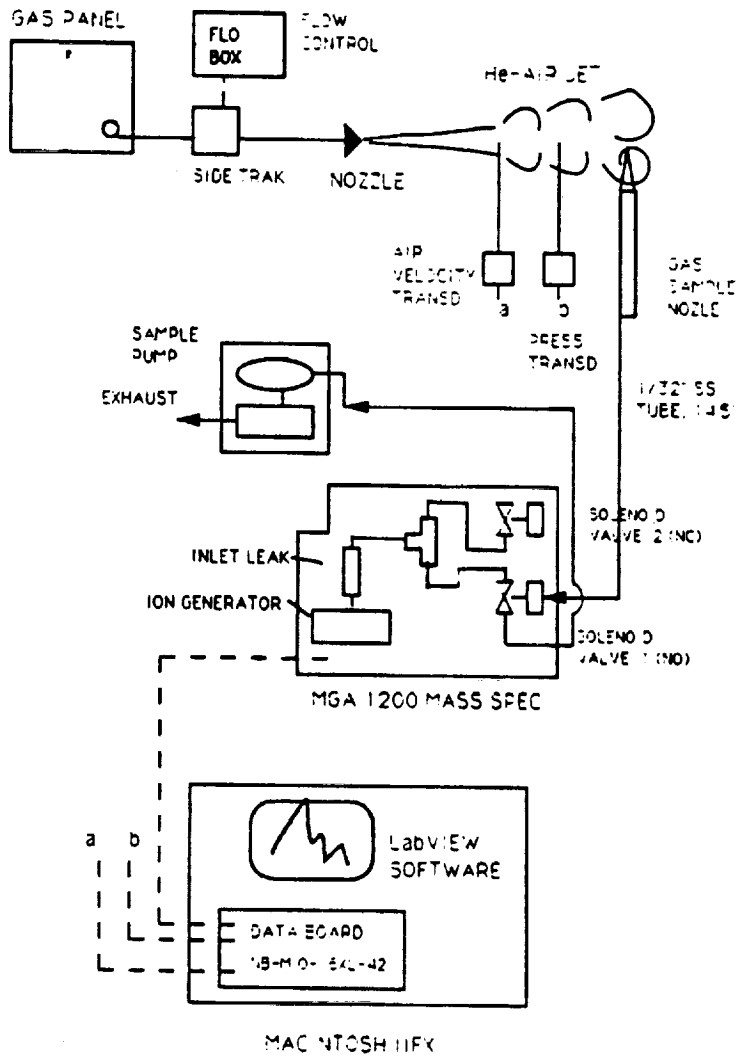


Figure 2. Present apparatus showing sample tube 3 arrangement

ORIGINAL PAGE IS OF POOR QUALITY

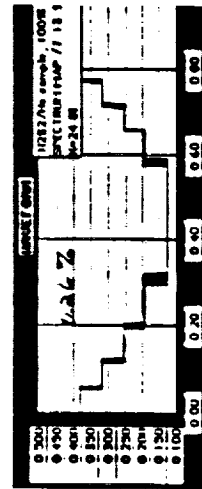
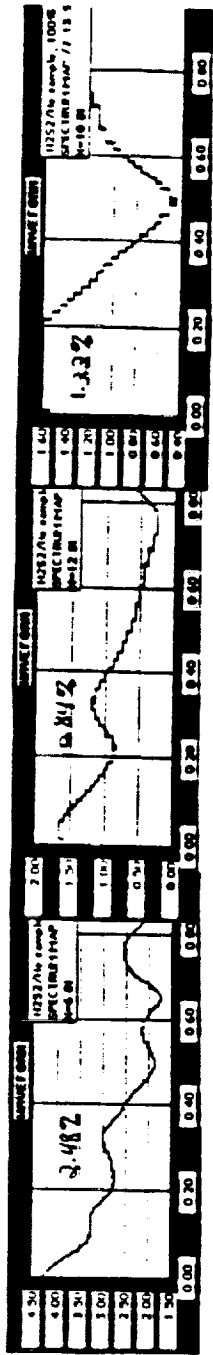
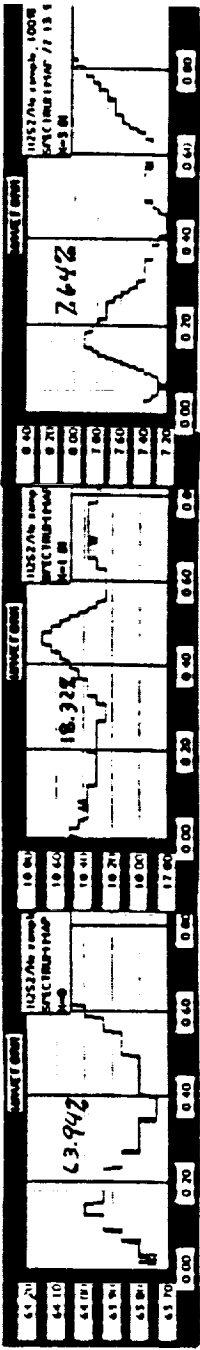


Figure 3b. GHe concentration vs. time, sec., at 7 values of x, 0 to 24 in.

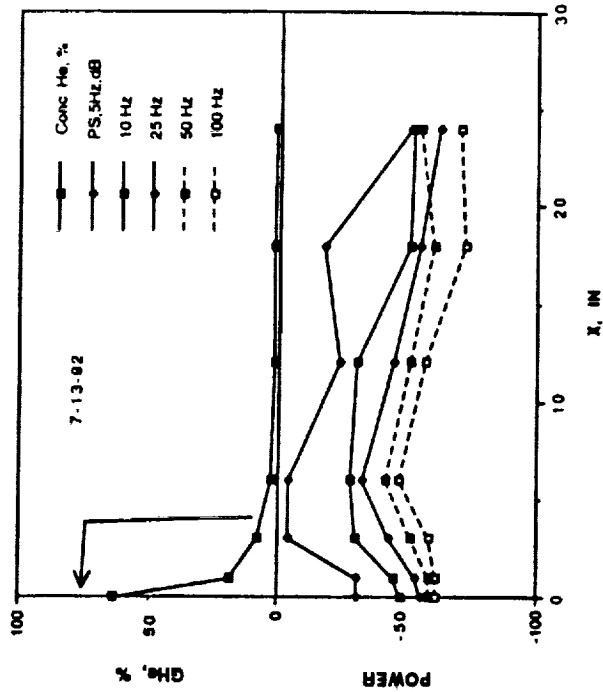


FIGURE 3a. GHe CONCENTRATION AND POWER VS. X. SONIC ORIFICE JET, 3.64 SLM, ST1.

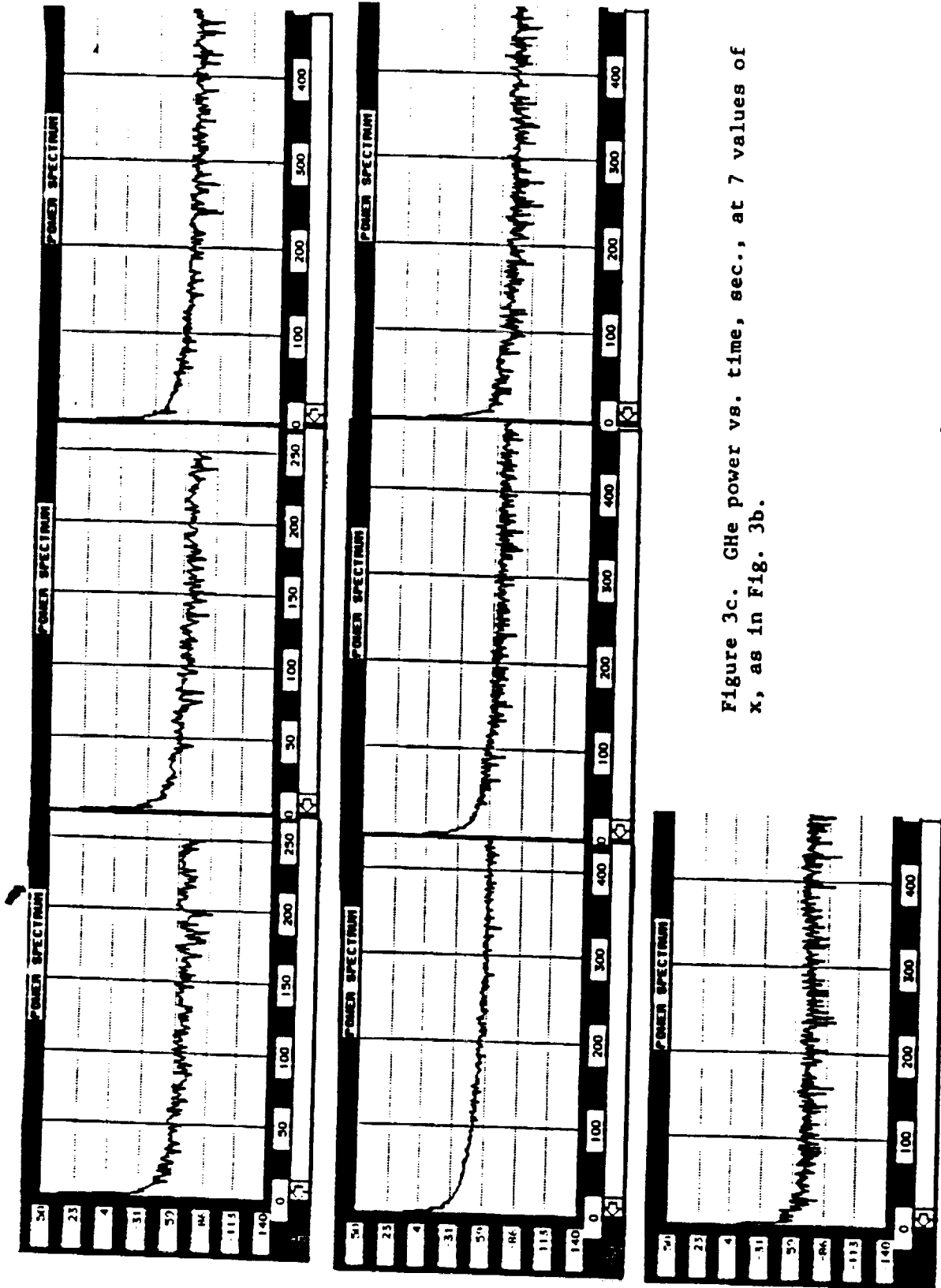


Figure 3c. GHe power vs. time, sec., at 7 values of x, as in Fig. 3b.

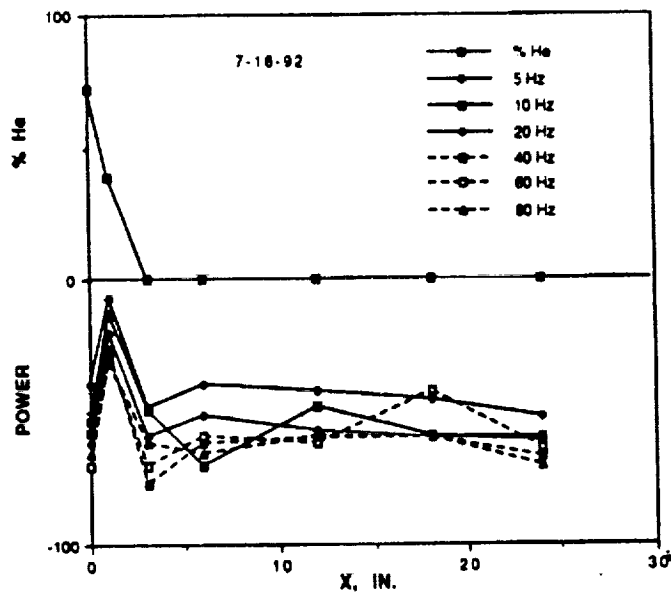


FIG. 4a. GHe CONCENTRATION AND POWER VS. X. TYGON TUBE JET, 3.64 SLM, ST1.

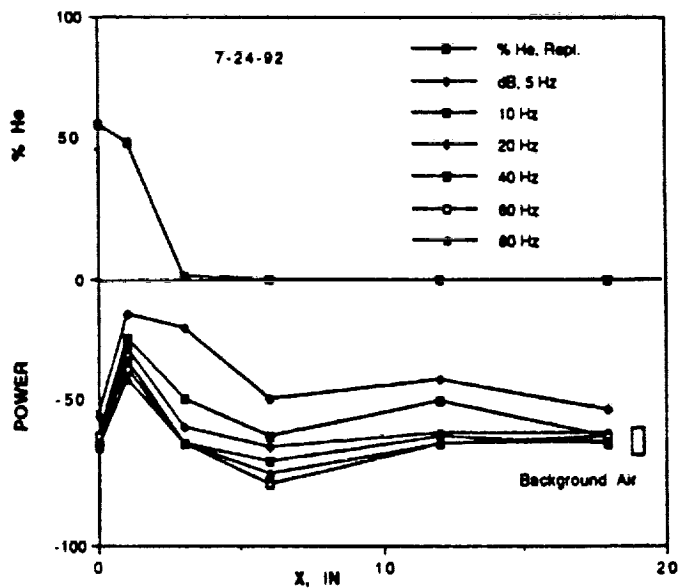


FIG. 4B. GHe CONCENTRATION AND POWER VS. X  
1/4 IN. TYGON TUBE JET, 3.64 SLM, REPLICATE

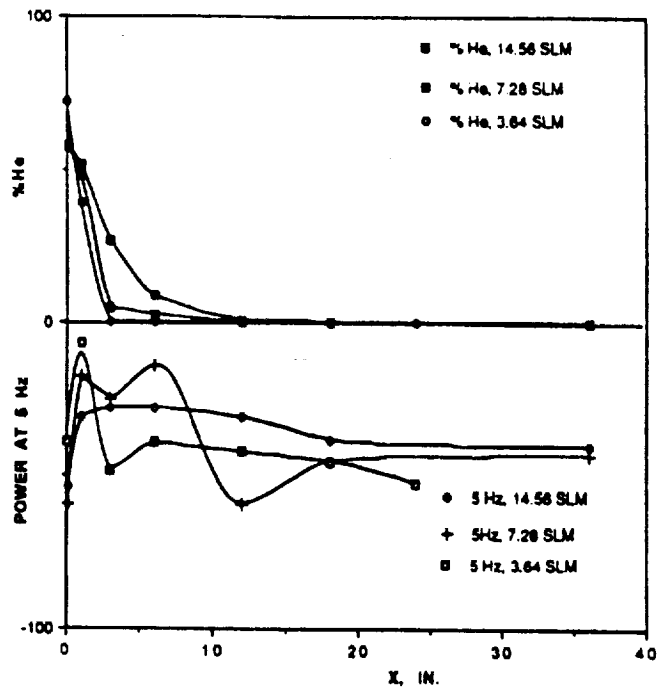


FIGURE 5. HELIUM CONCENTRATION VS. LENGTH, TYGON TUBE AT 3 FLOWS (ST1), 3.64, 7.28, 14.56 SLM GHe

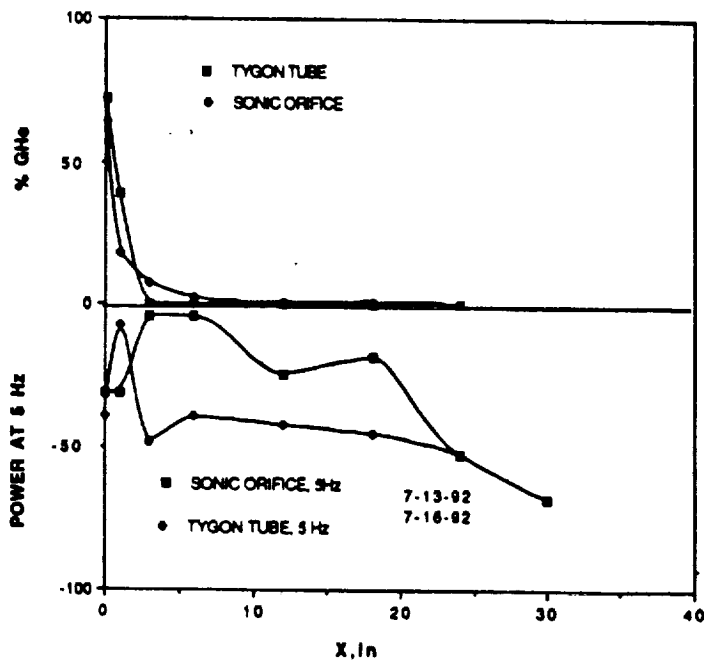


FIGURE 6. HELIUM CONCENTRATION AND POWER VS. X. COMPARISON OF SMALL (S.O.) AND LARGE (TYGON) ORIFICE AT 3.64 SLM.

GME JET, 3.64 SLM, 572 (OPEN SAMPLE TUBE, 1/32" ID) 8-7-92

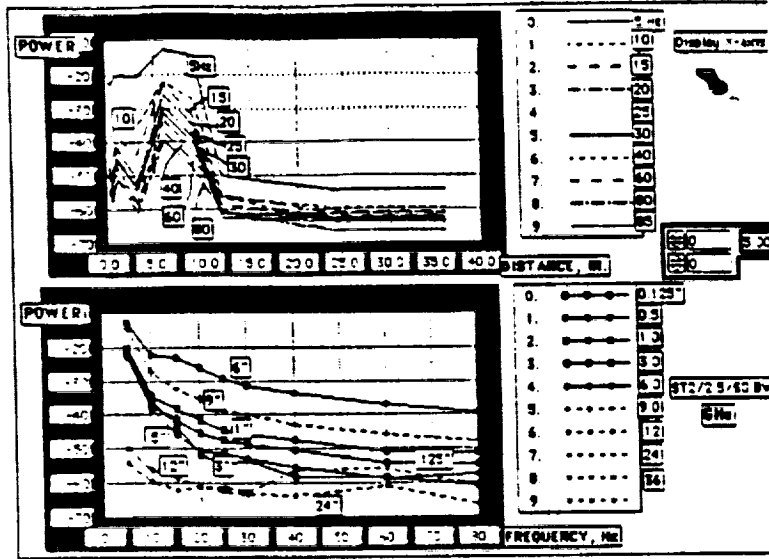


Figure 7. Power vs. length and frequency. Power is 10Hz bandwidth-averaged at center frequencies shown on top graph.

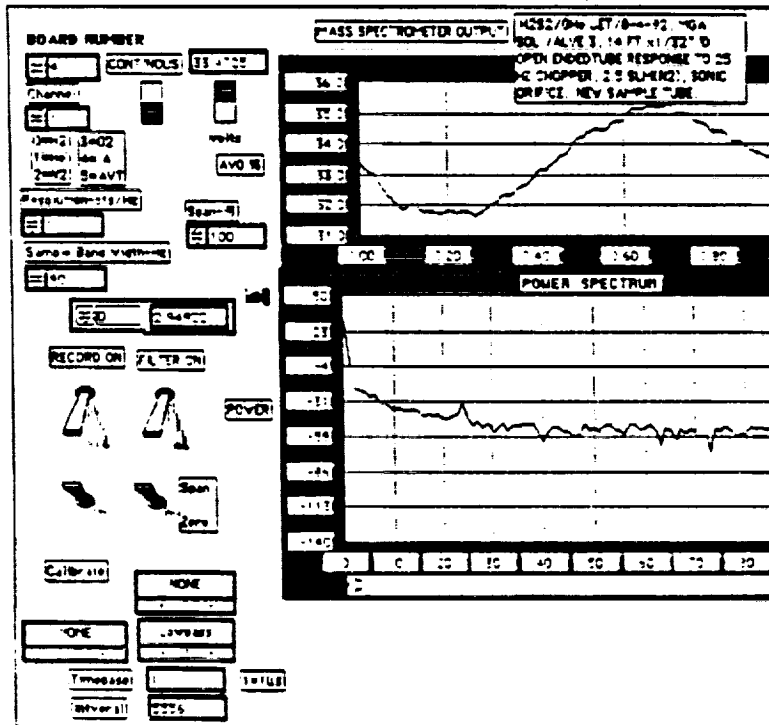


Figure 8. Mechanical chopper at 25Hz placed in jet stream 3 in. from orifice.

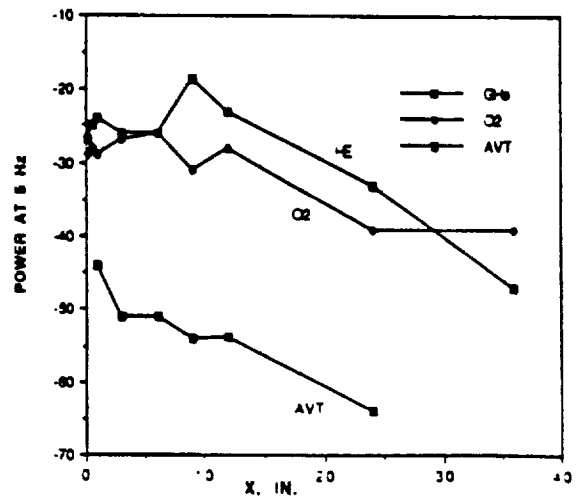
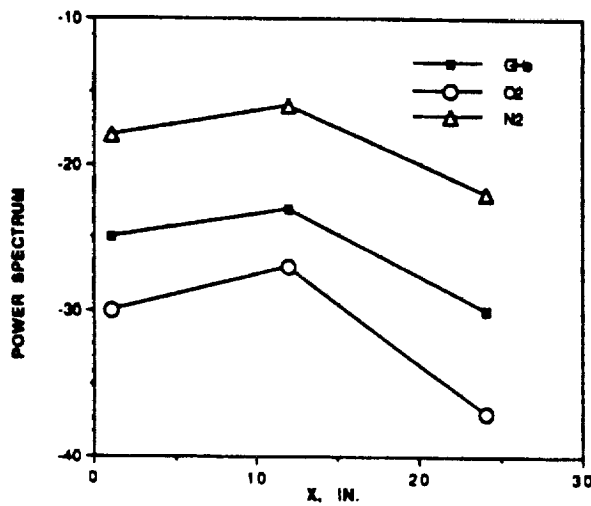
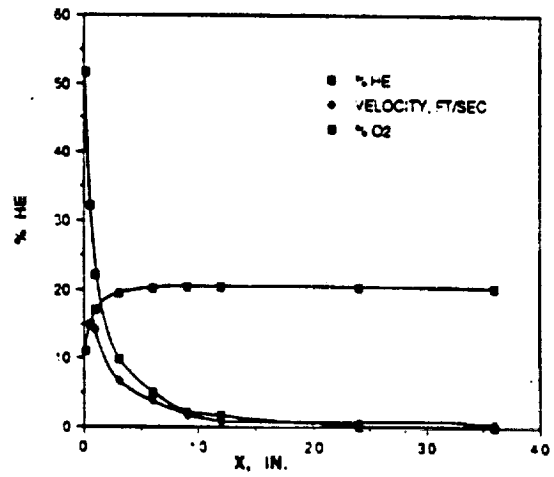
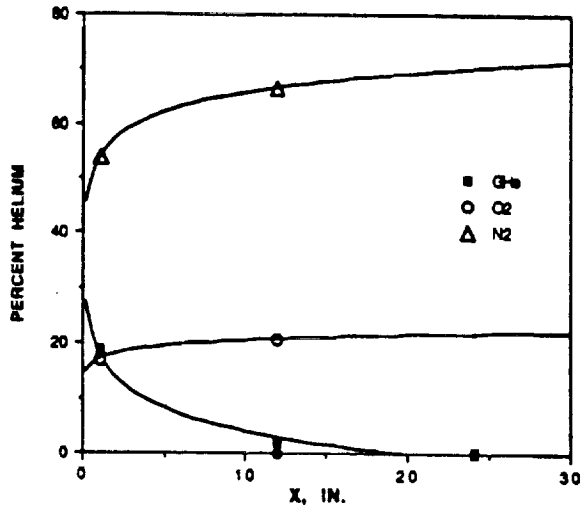


FIGURE 9. CONCENTRATION AND POWER @ 5Hz vs DISTANCE. COMPARISON OF GHe, O2, & N2. ST3/SO/ 3.64 SLM GHe.

FIGURE 10. VELOCITY AND POWER AT 5Hz VS X. COMPARISON OF GHe, O2, AND AVT. ST3. SONIC ORIFICE. 3.64 SLM GHe.

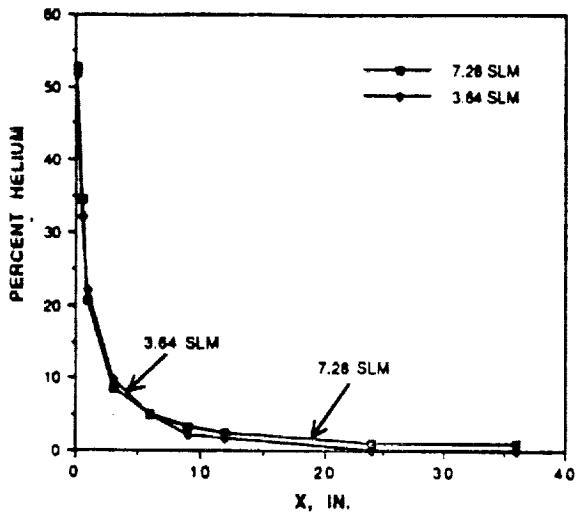


FIGURE 11. CONCENTRATION AND VELOCITY VS DISTANCE. COMPARISON OF 3.64 & 7.28 SLM GHe. ST3 SONIC ORIFICE.

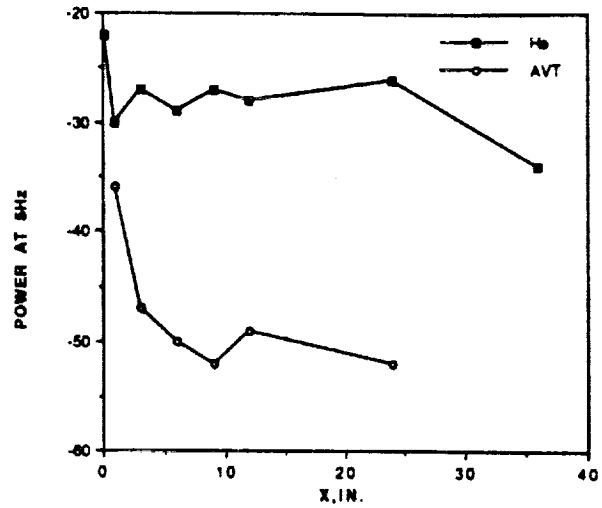


FIGURE 12. POWER AT 5 HZ VS. LENGTH. COMPARISON OF GHe & AVT DATA. ST3 SONIC ORIFICE, 7.28 SLM. GHe

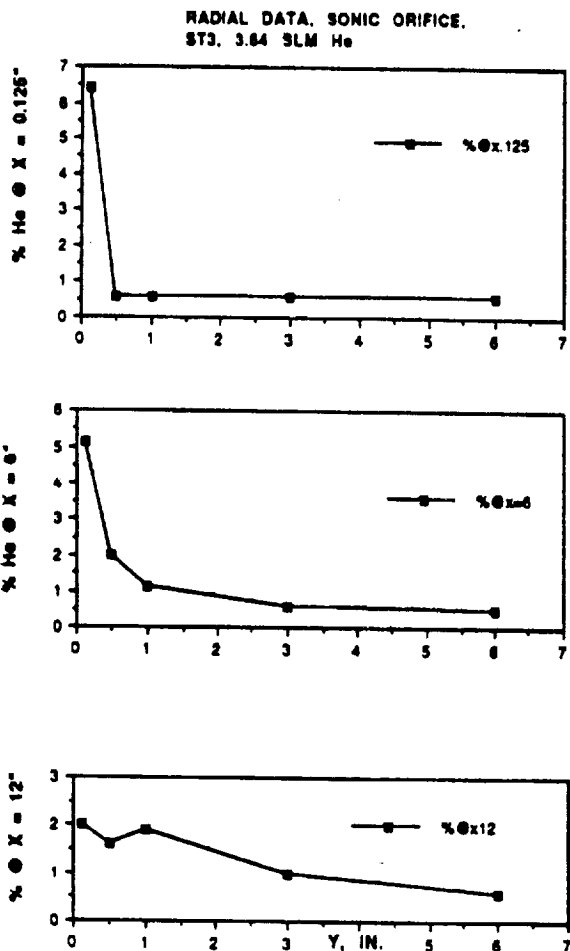


Figure 13. Helium concentration at three x values vs. radial coordinate y.

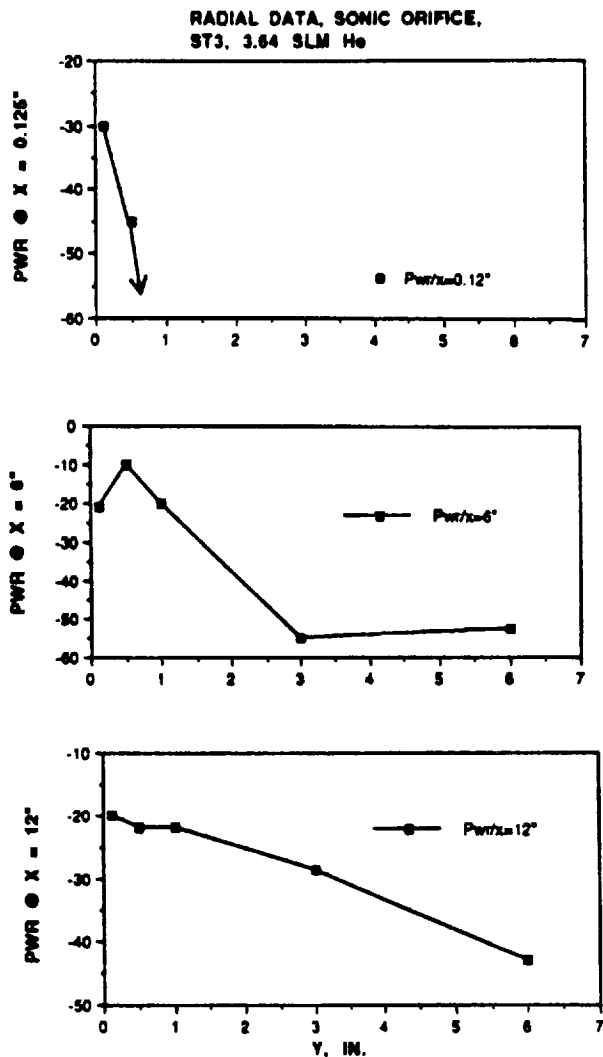


Figure 14. Power at 5 Hz, three x values, vs. y.

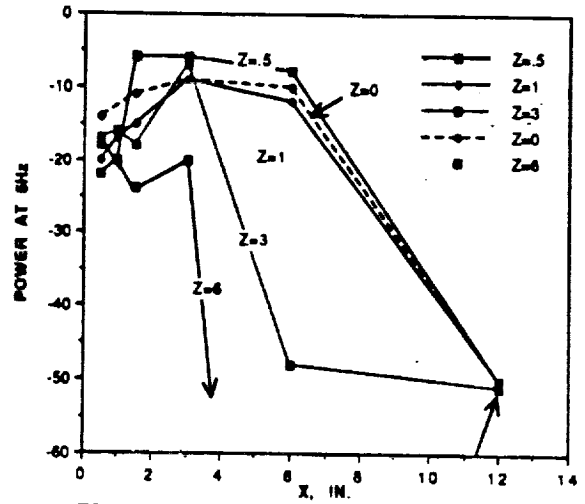
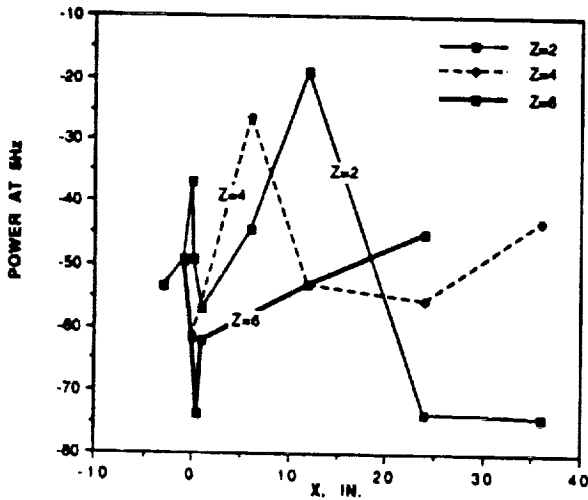
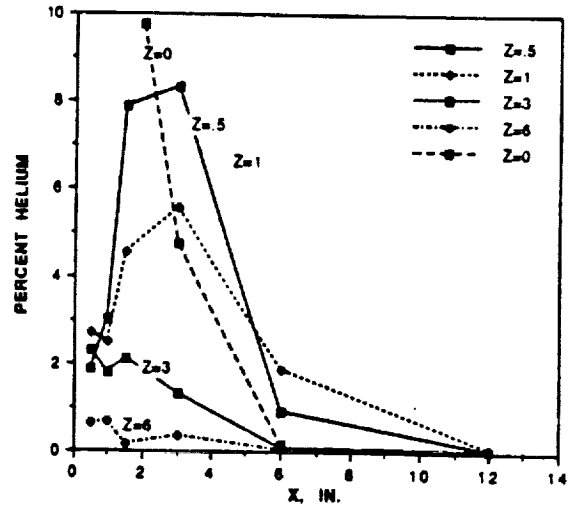
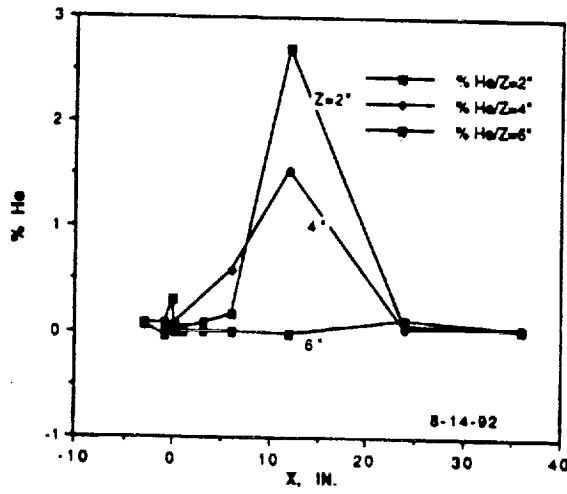


FIGURE 15. CONCENTRATION AND POWER AT 5 Hz VS. LENGTH. ST3, SONIC ORIFICE, 3.64 SLM GHe.

FIGURE 16. CONCENTRATION AND POWER VS LENGTH. HORIZONTAL CYLINDER OBSTRUCTION AT X = 1 IN. ST3, SONIC ORIFICE, 3.64 SLM GHe.

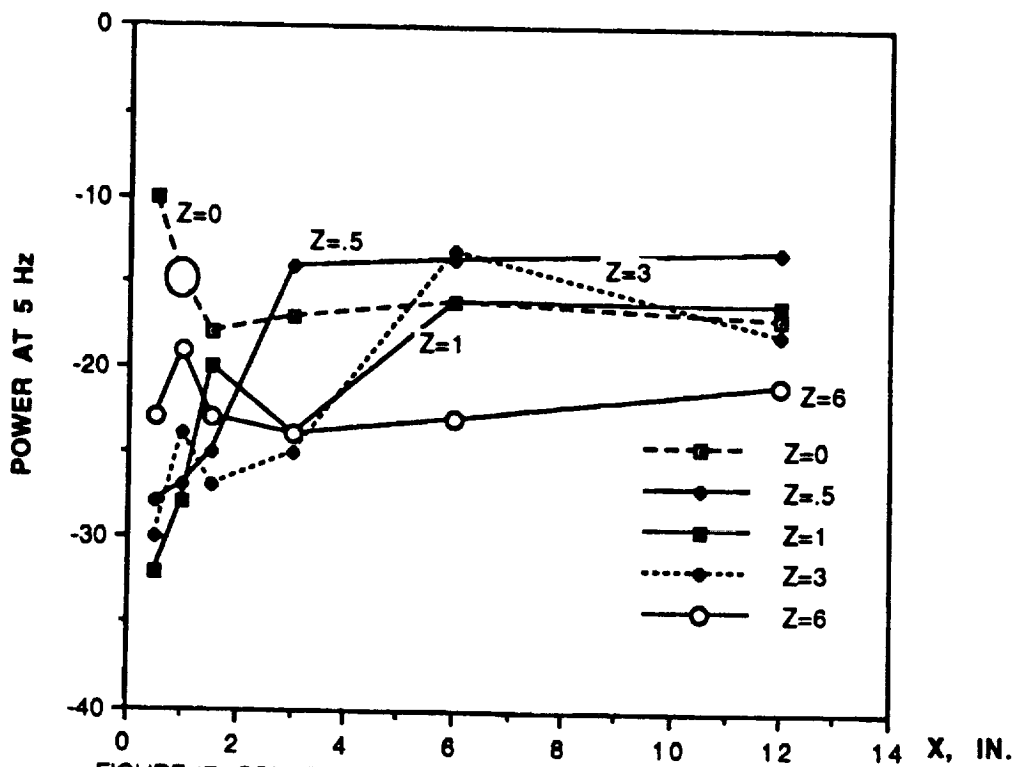
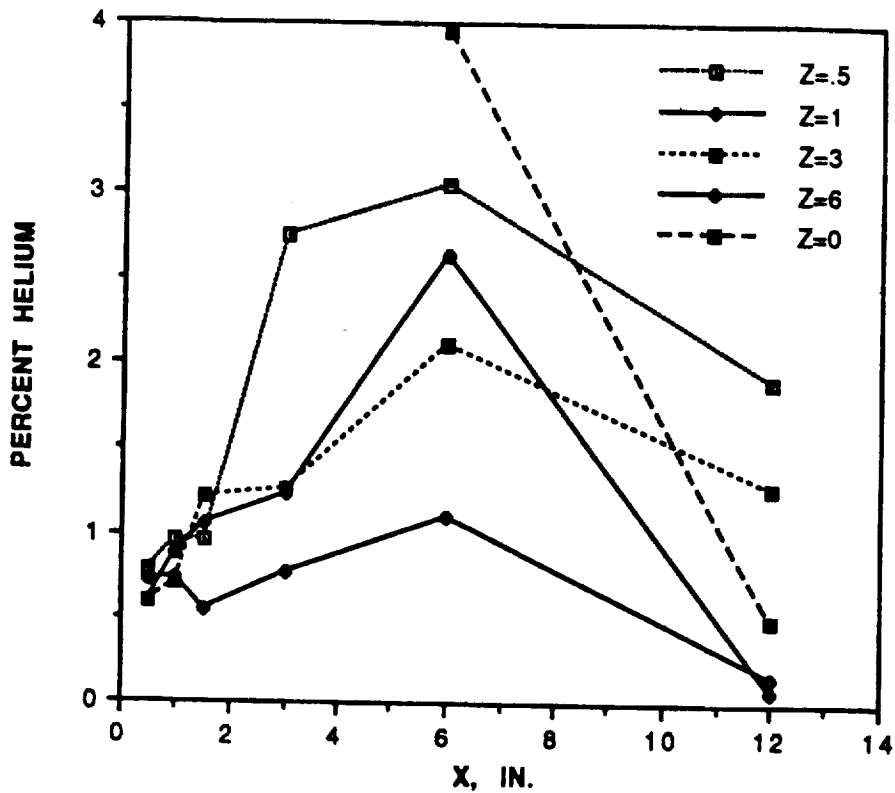


FIGURE 17. CONCENTRATION AND POWER VS. LENGTH.  
 HORIZONTAL CYLINDER OBSTRUCTION AT X=1 IN.  
 ST3, SONIC ORIFICE, 7.28 SLM GHe.

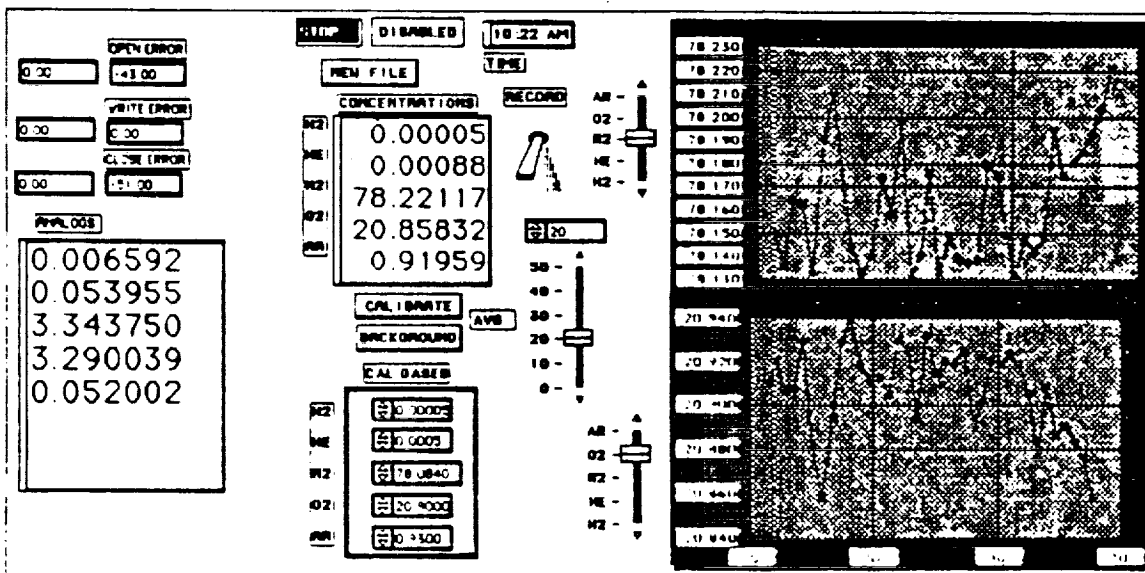
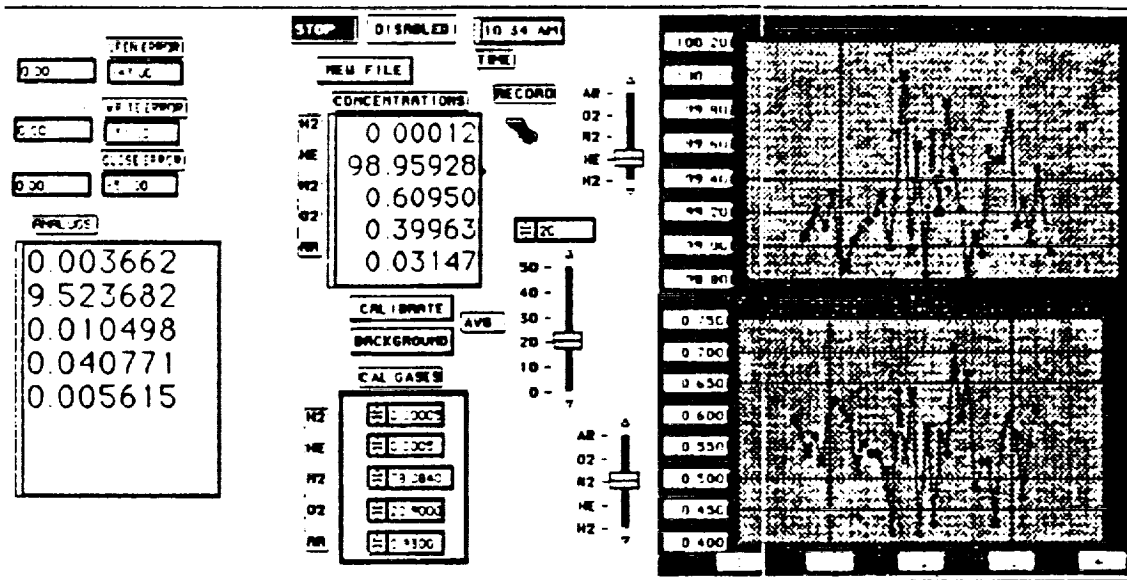
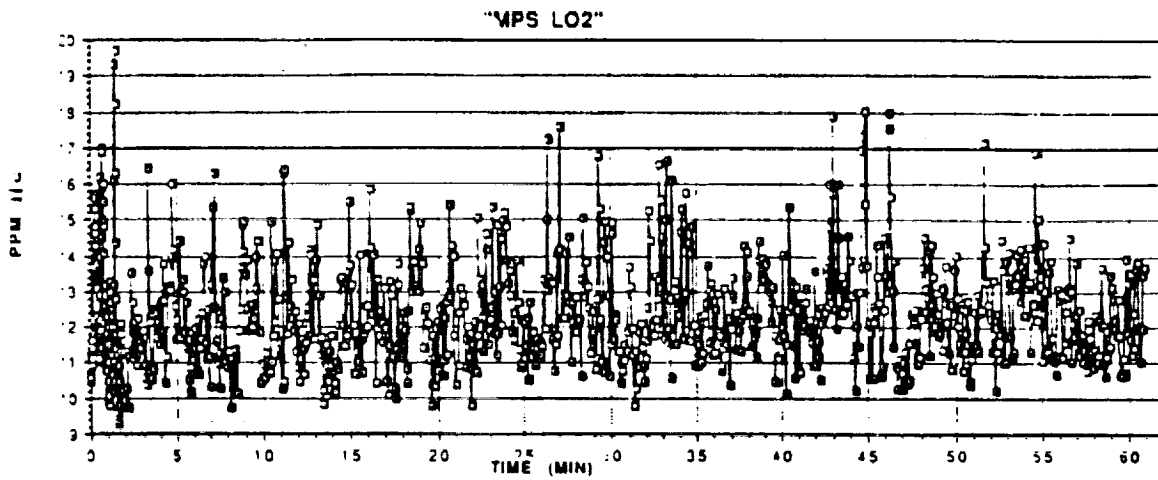


Figure 18. Top: helium (ppm) signature test in shuttle MPS; middle: helium (%) stream direct to mass spectrometer vs. time, sec.; bottom: stagnant lab air (%) vs. time, sec.